Multi-Terminal MVDC Grids Fault Location and Isolation

Mehdi Monadi [1*], Cosmin Koch-Ciobotaru [2], Alvaro Luna[1], Jose Ignacio Candela[1], Pedro Rodriguez[1,2]

[1] SEER Group, Technical University of Catalonia (UPC), Barcelona, Spain
[2] Abengoa Research, Seville, Spain

* mehdi.monadi@estudiant.upc.edu

Abstract: Voltage source converters (VSCs) are highly vulnerable to DC fault current; thus, protection is one of the most important concerns associated with the implementation of multi-terminal VSC-based DC networks. This paper proposes a protection strategy for medium voltage DC (MVDC) distribution systems. The strategy consists of a communication-assisted fault location method and a fault isolation scheme that provides an economic, fast and selective protection by means of using the minimum number of DC circuit breakers (DCCBs). This paper also introduces a backup protection which is activated if communication network fails. The effectiveness of the proposed protection strategy is analyzed through real-time simulation studies by use of the hardware in the loop (HIL) approach. Furthermore, the effects of fault isolation process on the connected loads are also investigated. The results show that the proposed strategy can effectively protect multi-terminal DC distribution networks and VSC stations against different types of faults.

1. Introduction

[1] The recent developments in VSC technologies have started to pave the way for the development of DC power systems in medium and high voltage levels [1]. These DC networks have several advantages over AC grids, such as the absence of skin effect, faster control of power flow, and the possibility to connect asynchronous AC systems [2-4]. Despite these advantages, DC networks introduce new challenges to the operational principles of power systems. Protection is one of the most important concerns associated with the VSC-based DC networks [5, 6]. This concern arises mainly due to the characteristics of the DC fault current which are quite different compared with the AC fault current.

Conventional AC circuit breakers (ACCBs) clear the fault during a zero crossing point of the current waveform; however, there is no natural zero crossing point for DC currents [7]. Thus, ACCBs are not applicable for interrupting the fault current in DC grids at their nominal voltage and current. Reference [8] suggested to interrupt the fault current in DC system by making use of the breakers in the AC-side of the VSCs. However, the typical ACCBs are not fast enough to interrupt the fault current before damaging the antiparallel diodes of the VSCs. In fact, the operation time of the medium voltage ACCBs typically is around several tens of milliseconds; whereas, DC fault currents must be interrupted in several milliseconds in order to protect the VSCs components [9]. Accordingly, works as the ones presented in [5, 9, 10] have suggested to place the DCCBs at each end of DC lines. However, DCCBs, in the medium and

high level of voltage, are more expensive than their counterpart AC; consequently, the suggested methods in [5, 9, 10] are not economically feasible for many distribution networks.

On the other hand, due to the low DC cable impedance, the rate of change of the DC fault current is very high [11]. Thus, the desirable fault discrimination is very challenging using the conventional overcurrent (O/C) relays [2]. In order to improve the performance of the conventional O/C relays in DC systems, the work performed in [12] suggested using the magnitude of DC-link voltage along with the fault current. A hybrid relay based on overcurrent and under-voltage elements has been also proposed in [13], where the relay sends the trip command when both the overcurrent and under-voltage element pick up. The work presented in [14] analyses the fault current derivative as opposed to its magnitude to estimate the fault location. Compare to the conventional overcurrent relays, these methods can provide a relatively improved performance in DC networks. However, they still rely on overcurrent-based element, which will increase the possibility of the protection failure when distributed generators (DGs) are integrated into the network [3].

The work presented in [9] has proposed a distance protection for MVDC networks. In this method, faults in DC systems are located by estimating the distance from the fault point to the location of the relay. However, the main challenge associated with this technique is the impact of fault impedance on the accuracy of the method, particularly for short distribution lines. In another similar method, the equivalent impedance from the fault point to the relay location is estimated by an active impedance estimation method [15]. In this method, a spread frequency current is injected to the DC feeder and the resultant voltage is recorded. The measured voltage and current are then used to calculate the equivalent impedance. However, the choice of a proper frequency for the injected current and the impact of fault impedance are the main issues of this method.

Several signal-processing-based methods have been also suggested for the protection of DC systems. For example, an artificial neural network (ANN)-based fault location has proposed in [16]. In this method, to determine the fault location, the sampled voltage and current are fed to the ANN, directly. However, the directly use of these quantities, not only increase the required time for the learning process, but it also increases the possibility of protection mal-operation due to the noise and incorrect sampling [5, 17]. Hence, the authors in [17] have suggested using the wavelet transform to extract a feature vector for the measured quantities. This vector then is introduced to an ANN-based fault locator. Also, in [5], faults in DC networks are detected by analyzing the wavelet-transform coefficients of voltage and current along with the magnitude and derivative of the DC bus voltage. However, in wavelet/ ANN-based methods, specific features of the voltage and current waveforms should be extracted to detect and/or locate network faults. Since the extracted features are not necessarily the same for all DC systems, these methods cannot provide

a generic approach for the protection of DC networks. Indeed, a major disadvantage of such methods is that they must be re-designed based on the characteristics of each distribution feeder. Moreover, the need to a relatively faster protection algorithm in DC systems limits the application of signal-processing-based method in these networks [10].

The travelling-waves-based methods has been also suggested to protect DC lines. For instance, in [18] it is suggested to locate DC faults by calculating the difference in arrival times of the travelling waves to both ends of the faulty line. However, due to the small length of distribution feeders, it is very difficult to obtain the exact time difference and determine the exact location of the fault. In addition, in [19] faults are located by analyzing the specification of the travelling waves. However, this method is suitable for long transmission lines where specifications of travelling waves are significantly different when a fault happens inside or outside the protected line.

On the other hand, communication-assisted methods can provide fast and selective protection strategies without using any complex algorithm. For example, differential protection has been used in [20, 21] where the measured value of the current at one end of the protected line is transmitted to the other end through communication links. However, the potential need for synchronized measurements in both sides of the protected line is an important issue about the implementation of differential method for power lines. Furthermore, since thresholds of the differential relays are set on a smaller value than thresholds of O/C relays, there is a higher risk of relay malfunction caused by measurement error or communication issues.

The proposed protection strategy consists of a fault location method and a fault isolation scheme. Compared with presented methods in the previous literature, the main aspects of the proposed strategy are:

1- The proposed fault location is an adaptive-communication-assisted method based on the directional-overcurrent protection. In this fast and selective protection scheme, faults are located by use of the exchanged signals among the relays installed at both sides of lines. Accordingly, the fault location method does not rely on the synchronized measured current from both sides of the protected line.

2- The proposed method can provide a generic protection method without using the time-consuming and complex methods. Moreover, high rising rate of DC fault currents, change in the network topology, and intermittent behavior of DGs cannot cause protection mal-operation.

3- To manage communication failures, the proposed scheme is equipped with a backup fault location method that is activated if communication system fails.

4- The proposed protection scheme has been implemented and tested in real-time using the OPAL-RT real-time simulator; thus, some of the practical concerns, like communication delay, have been taken into account, leading to a more accurate verification.

Furthermore, the paper implements an economic advantageous fault isolation scheme based on the

coordinated operation of isolator switches and DCCBs. Since the fault isolation scheme includes a network restoration process, the effects of this strategy on the connected loads has also investigated.

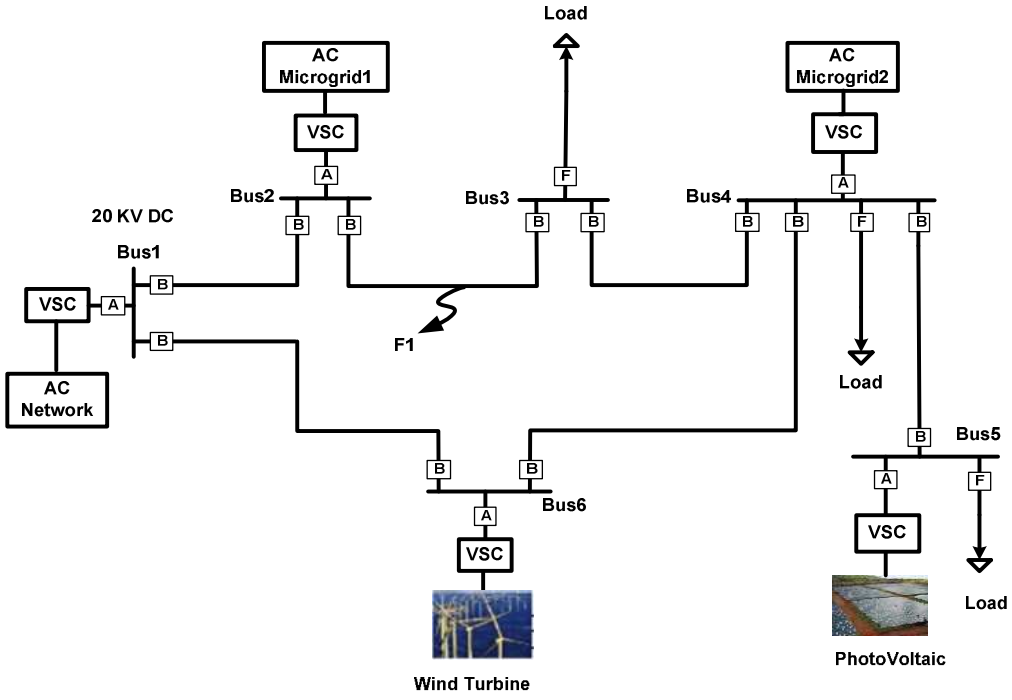

Fig. 1. *A prototype multi-terminal MVDC network.*

2. MVDC Distribution System Study Case

Different applications are introduced for MVDC networks such as: connection of AC microgrids and creation of multiple-microgrids [22], connection of renewable energy sources (RESs) to grids [23], increasing the transmission capacity of the existing AC lines by conversion to DC [24, 25], and simple integration of DC loads (especially in industrial applications) [26]. Fig. 1 shows a hypothetical multi-terminal DC distribution network which is designed to handle these applications. Hereafter, the network of Fig.1 is referred to as the "*study network*".

The study network is a bipolar system consisting of radial and loop lines. The ±10kV VSCs are used to interface the AC network, microgrids, and RESs to the DC network. All the VSCs have two-level topology using sinusoidal pulse with modulation (PWM). The voltage level of this grid is controlled by the controller of VSC1. Thus, VSC1 is in voltage control mode and the other VSCs are in power control mode. In addition to the external protection, the VSCs are equipped with the internal protection in order to protect the main switches (i.e., IGBTs). The internal protection blocks the main switches if their current exceeds the predetermined threshold. Moreover, the Hall-Effect current-transducers (CTs) are installed at each side of DC lines and busbars. The data transmission between all the DC busbars is performed through dedicated communication links. The integrated loads and microgrids data as well as the cable parameters, are reported in Tables 2 and 3 of the Appendix.

3. Requirements of The Proposed Protection Strategy

Protection schemes for the VSC-based DC networks should be designed according to the specification of the fault current in such networks. Components of DC faults are *i*) the DC link capacitors discharge current (i_C), *ii*) the cable inductance discharge through the freewheeling diodes (i_L), and *iii*) the ac-grid current (i_{Grid}) [3]. The VSCs do not participate in the fault during the capacitor discharging period, and hence initially they remain safe. However, further on, the inner controller of the VSCs blocks the main switches and then the fault current flows through the freewheeling diodes. This current can quickly damage the freewheeling diodes. Consequently, a system designed to protect the VSC-based DC grids, should break the fault current during the capacitor discharging period. Indeed, the moment of starting the second component of the DC fault is the critical time of the fault current interruption. Accordingly, the proposed protection strategy is designed to protect the MVDC distribution networks by use of the following components.

3.1. Fault clearance by use of DCCBs

As mentioned on Section 1, DCCBs are necessary to interrupt the fault current and protect the VSCs against faults in DC networks. On the other hand, once a fault impacts a DC network, the fault current can be supplied by the AC-side sources, DGs, and microgrids. Therefore, the fault current can be interrupted if the DCCBs are located only at the connection points of these active elements to the network (points tagged as "A" in Fig. 1).

Solid state CBs (SSCBs) are able to operate in less than 1 millisecond [27]; however, these CBs are lossy devices [28]. To improve the efficiency of SSCBs, hybrid-type CDCBs were presented that are able to interrupt fault currents in less than 5ms [29]. Therefore, the DCCBs which are used in this paper were simulated based on the specifications of the hybrid type DCCBs presented in [29]. The operational aspects of these type of breakers and their components were explained in [30]. In the proposed strategy it is assumed that hybrid DCCBs are installed at points "A" of Fig 1.

3.2. Fault detection by overcurrent-based local protection unit (LPU)

Due to the fast rising rate of DC fault currents, fast fault detection can be obtained by monitoring the current flowing from the VSC stations to the connection points of the network. Therefore, a "local protection unit" (LPU) is installed at each connection point wherever DCCBs are placed. The LPU includes an instantaneous overcurrent unit which operates according to a predetermined threshold and the current flowing through the connection point. The LPU detects the solid faults within several tens of microseconds and sends the trip command to the corresponding DCCB, as its main function. The LPU also communicates with the other protection devices to handle the other functions that are explained in Section 4.

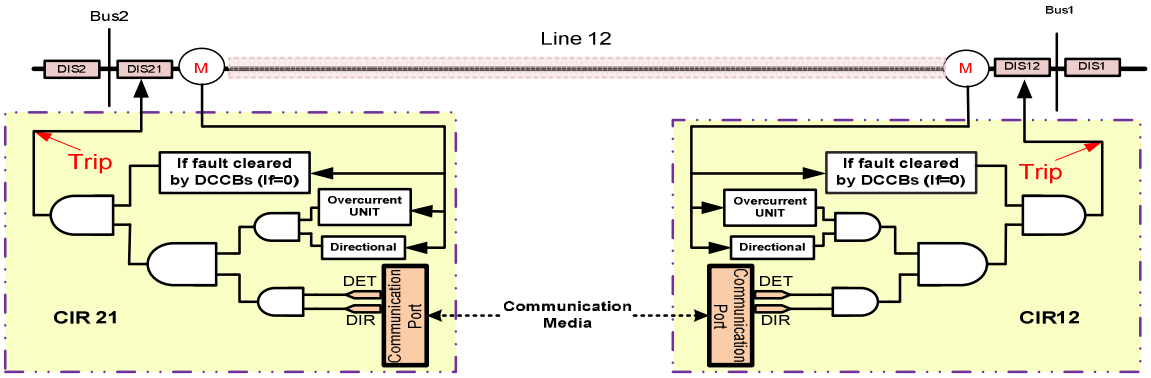

a.

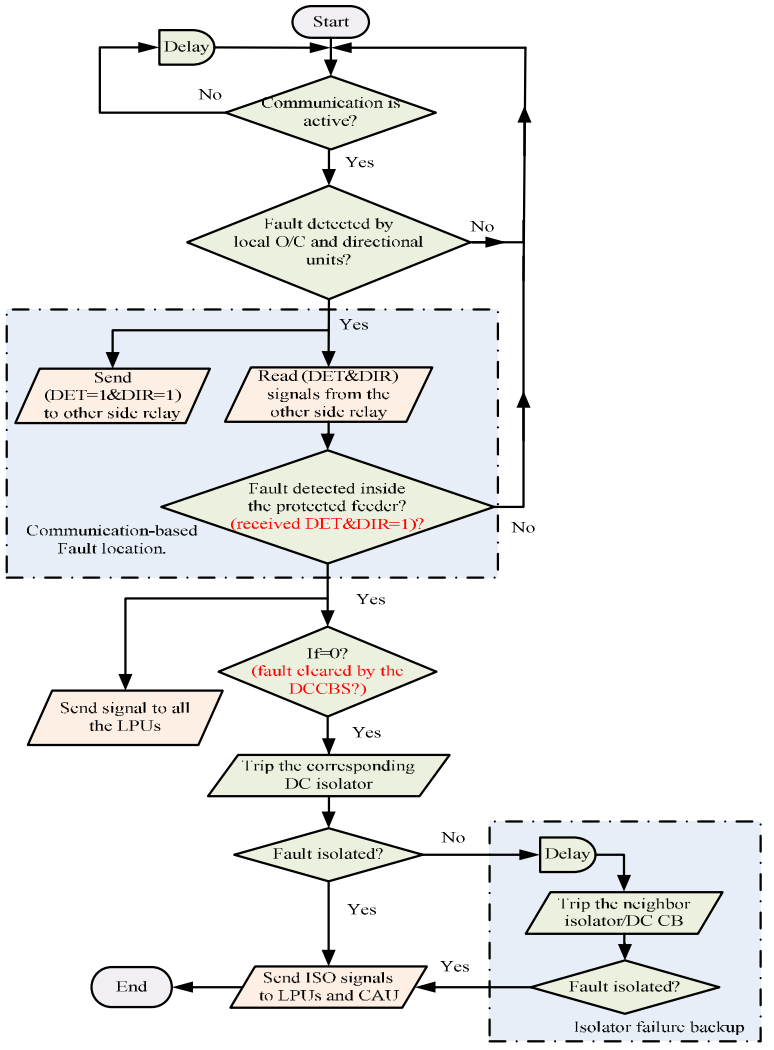

b.

Fig. 2. *The logic circuit and the flowchart of the proposed CIR.*
a. The logic circuit.
b. Flowchart.

3.3. Fault isolation by use of the isolator switches

To isolate the faulty parts of the MVDC network and facilitate the network restoration, DC isolator switches are placed at each end of the lines. This type of switches, which are considerably cheaper than DCCBs, must be opened/ closed when their current is close to zero. Therefore, they are used to isolate faulty parts after the fault current interruption by the DCCBs. The conventional ACCBs can be an appropriate choice for this purpose [31].

3.4. Fault location by use of the CIR

To locate the exact faulty line, a "communication-assisted isolator relay" (CIR) is implemented in this paper. The CIRs are equipped with instantaneous-overcurrent and directional units, as it is shown in the logic circuit of Fig. 2.a. The directional unit can detect the direction of fault currents knowing the placement and connections of the corresponding CT as well as the sign of its digital output. If a fault impacts a line, fault currents flow from both end of the line to the fault point; thus, the faulty line can be detected by use of the exchange signals among the relays installed at both ends of the line. Fig. 2.a indicates that each CIR receives two signals from another CIR installed at the other end of the corresponding line. These signals are: *i*) the DET signal that determines the fault detection by the relay and *ii*) the DIR signal which determines the fault current direction. Table 1 represents the meaning of DET and the DIR signals when their value is "0" or "1".

The flowchart of Fig. 2.b provides a graphical illustration of the proposed algorithm for the CIRs. This flowchart shows that if the overcurrent unit of a CIR detects a fault and its directional unit confirms that the fault current is flowing from bus to line, the CIR will change the value of its DER and DIR signal to "1" and sends these signals to the CIR installed at the other end of the line. Then, if the CIR receives DET=1 and DIR=1 from the other end CIR, it will recognize that the fault has occurred inside the protected line. In this case, the CIR will send the open command to the corresponding isolator after the fault current interruption. The other roles of the CIRs are explained in Section 4.

It is also worth noting that, since each DC line consists of a positive and a negative pole, the CIRs of each line, receive the measured currents of both poles of that line. Moreover, the number of the CIRs installed at the station of each bus is related to the number of DC lines connected to that bus.

Table 1. Meaning of the exchanged signals among CIRs

Signal value / Signal name	**1**	**0**
Fault Detection (DET)	Fault detected by the O/C unit	Normal condition
Current Direction (DIR)	Inside: from bus to line	Outside: from line to bus

4. Proposed Protection Strategy

This section explains the proposed protection strategy given the protection elements described in the

Section 3. The proposed strategy includes both main and backup methods. The main protection is communication-assisted; whereas, the backup protection is activated when the communication link fails.

4.1. Main Fault Location Method

In this strategy, the connection points are equipped with DCCBs and LPUs. The isolator switches and the CIRs are also installed at DC feeders, as shown in Fig. 3. The operation sequence of the main protection is explained here according to the time sequence shown in Fig. 4.a.

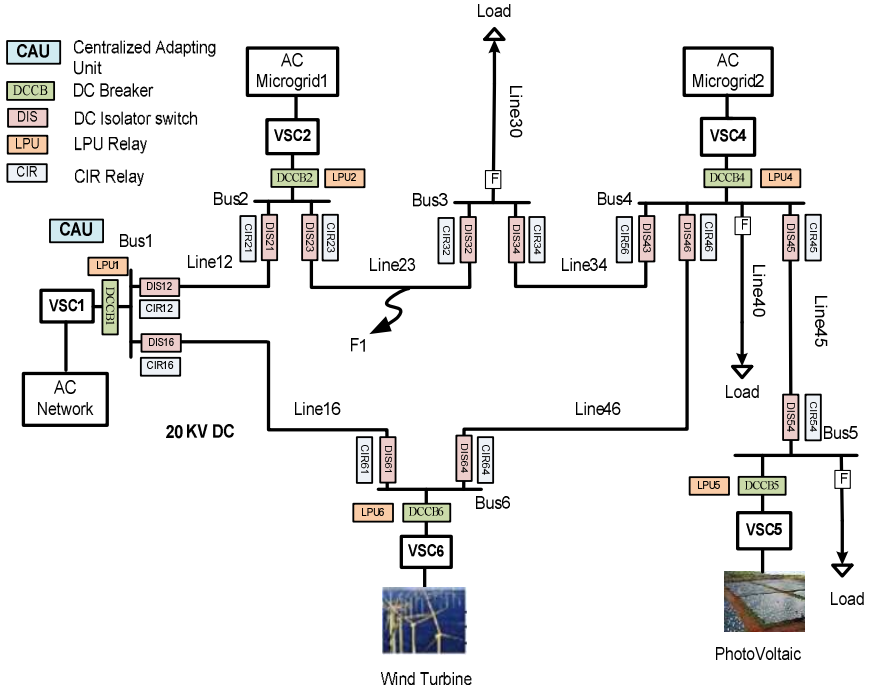

Fig. 3. *Study network with the protection elements.*

Subsequent to the fault occurrence, the LPUs detect the fault and send the trip command to the associated DCCBs at $t = t_1$. At the same moment, each CIR starts sending the DET and the DIR signals to the CIR located at the other end of its corresponding line. The DCCBs operates and interrupts the fault at t_3. Simultaneously with the operation of the DCCBs, the DET and the DIR signals are transmitted among the CIRs. Therefore, considering the communication delay, i.e., $t_1 - t_2$, the faulty line is detected at t_2. Then, the CIR, installed at each end of the faulty line, monitors the line current and sends the open command to the associated isolator when the fault current decays to zero. During $(t_4 - t_5)$ the isolators operate and then the faulty line is isolated at t_5. Finally, the LPUs send the close command to the corresponding DCCBs and the network is restored. Fig. 4.b show the algorithm of the LPUs, which can be implemented on a microprocessor-based relay.

It is also notable that since the pickup current of the LPUs is typically larger than those of CIRs, the possibility of the high impedance fault (HIF) detection by the CIRs is higher than the fault detection probability of the LPUs. Therefore, after the fault detection by the CIRs, they will send the appropriate

notification signals to the LPUs to increase the possibility of the HIF detection. Indeed, although the LPUs, as the main fault detection unit, can detect the solid/ low-impedance faults faster than the CIRs, sending this notification signal can improve their performance in the case of HIF occurrence and consequently can enhance the protection reliability.

The proposed protection strategy is summarized as the following steps:

1. The fault is detected by the LPUs and the trip command is sent to the DCCBs.
2. The DCCBs interrupt the fault current.
3. The location of the fault is determined by the CIRs.
4. The faulty line is isolated by opening the corresponding isolator switches.
5. DCCBs are re-closed; the rest of the network is restored.

It should be noted that during the above steps, microgrids can operate in grid-isolated mode. Therefore, if there is a power balance between the generation of the internal DGs and the connected loads inside the microgrid, these loads will not sense any interruption (see Section 8).

4.2. Backup Fault Location Method

When the communication system is interrupted, the CIRs cannot locate the fault; hence, their operation is blocked. On the other hand, as shown in Fig.4.b, the LPUs are switched to the backup strategy, which does not require communication. The algorithm of the backup strategy is designed based on the handshaking method presented in [8] with major modifications in order to improve its performance. The proposed backup protection, which can be named as modified handshaking method, is explained here in the context of the study network, shown previously in Fig. 3.

Let us assume that fault F1 impacts Line23 when the communication link has failed. In this case, the LPUs detect the fault and send the trip command to the DCCBs. Furthermore, before the fault current interruption, the LPU of each active bus determines the isolator that carries the maximum fault current flowing from the bus to the lines (i.e., maximum positive current); these isolators are named “selected isolators”. When the fault current is interrupted, the selected isolator of each active bus is opened. For example, in the study network, DIS23, DIS12, DIS61, DIS54 and DIS43 are opened after the fault interruption.

By opening the selected isolators, the faulty part is isolated; however, in order to provide a selective protection, most of these switches must be re-closed. To recognize the candidates for re-closing, the DCCBs are re-closed whereas the opened switches are still open. At this stage, the opened isolators that have both their poles connected to the energized bus, i.e., DIS12, DIS61, DIS54 are selected; these switches are allowed to be re-closed. To guarantee the safety of the isolators, these switches are re-closed when the network is de-energized. Therefore, once the candidate of re-closing is selected, the LPUs send

open commands to the DCCBs, again. Consequent to the opening of the DCCBs and de-energizing the network, the candidate isolators are re-closed. Finally, the DCCBs receive close commands and restore the rest of the network.

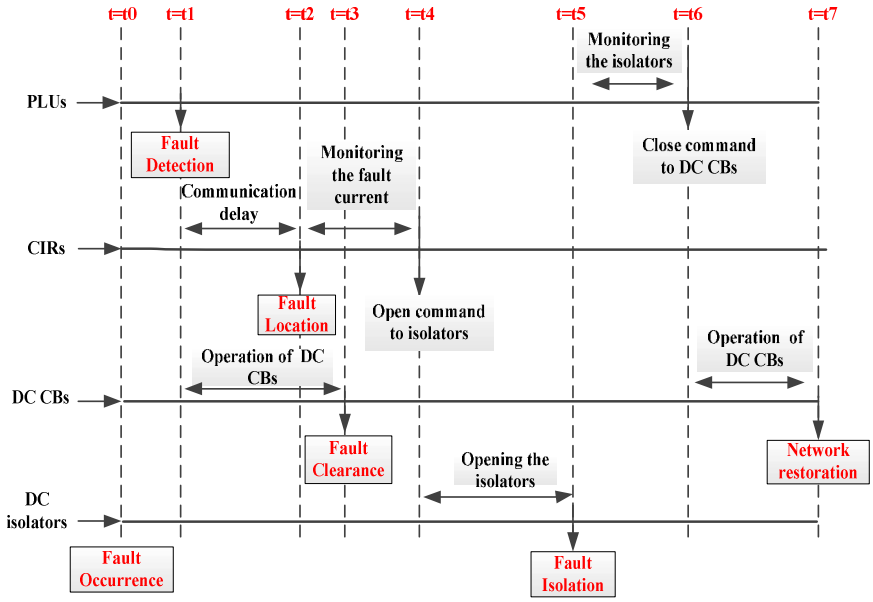

a.

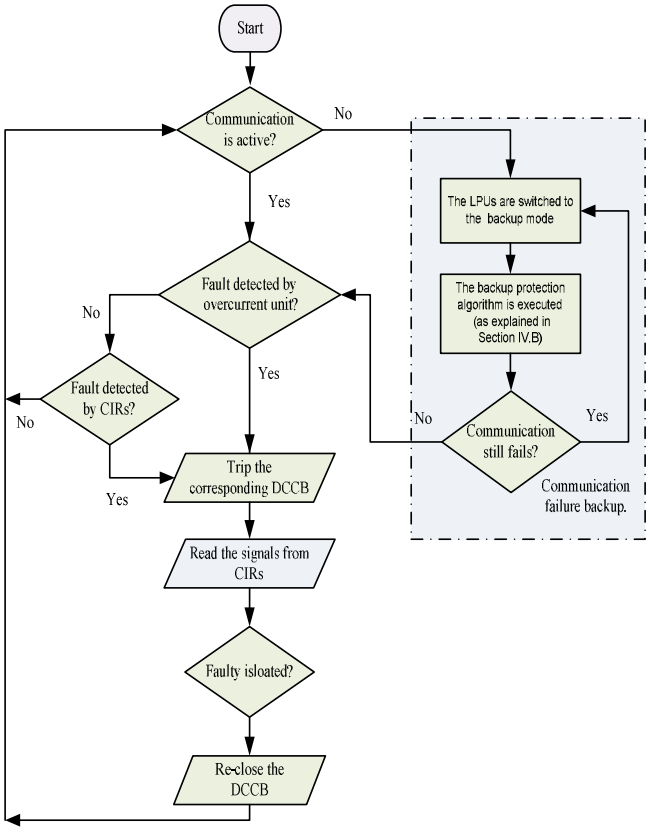

b.

Fig. 4. *The proposed protection strategy.*
a. The time sequence of the main protection when a solid fault occurs at t_0 .
b. Flowchart of the proposed algorithm for LPUs.

Steps of the backup method are:

1. The fault is detected by the LPUs and the trip command is sent to the DCCBs.
2. The LPU of each bus detect the isolator that carries the maximum positive fault current.
3. The DCCBs interrupt the fault current.
4. The open command is sent to isolators selected in Step (2), when the current flowing through the isolator decays to zero.
5. The isolator switches selected in step (2) are opened.
6. The DCCBs are re-closed when the selected isolators are opened.
7. Isolators that should be reclosed are selected.
8. The DCCBs are re-opened.
9. The isolators selected in step (7) are re-closed.
10. The DCCBs are re-closed and the rest of the network is restored.

Compared to the main protection, the backup causes a larger time delay in network restoration; this issue is explained in Section 7.2 (Case Study2).

As mentioned above, in Step (2) of the backup method, the LPU of each bus selects the isolator that carries the maximum positive current. In a special case, if the measured currents of two isolators of a bus are equal, both of them should be selected in Step (2). Therefore, after opening the DCCBs, both these isolators are opened. The rest of the steps are executed as mentioned above. Indeed, even for this special case, the method is still stable. Both isolators can be re-closed in Step (9) if the fault is not located inside their corresponding line.

It is also notable that, after the activation of the backup protection, the isolator failure backup is handled by the LPUs. For example, after the fault occurrence in Line16, the LPU6 sends the open command to DIS61 (Step 4). If DIS61 fails to open, the LPU6 will detect this failure and sends the open command to DIS64 after a time interval. In this case, after the fault isolation, the LPU6 will not send the close command to the DCCB6.

4.3. Busbar Protection

Once a fault occurs at a bus, the fault currents flow from feeders to the faulty bus; thus, the CIRs cannot locate the fault. For this reason and also due to the requirement of a more sensitive protection, the busbar protection is designed based on the differential current method. The differential protection is used typically for busbar protection due to its high selectivity and fast operation [32]. In this paper, the busbar protection is considered as a function of the LPUs; however, for the buses without a LPU, an independent relay should be allocated.

5. Adapting The Relays Thresholds

The LPUs and the CIRs detect faults based on the overcurrent method. The operation of the overcurrent-based relays is related to the time-dial and the pickup current (I_P) settings. Considering the use of the instantaneous overcurrent units, the proposed relays operate without time delay. Meanwhile, the upper limit of the pickup current of each relay is selected according to the nominal current of the corresponding VSC station and/or the capacity of the protected line. Also, the pickup current should be selected higher than the nominal current of the protected line to prevent unnecessary operation of the protection system. Thus, the lower limit of the pickup current is determined according to the nominal current of the protected line. It is worth noting that, to prevent the relay mal-function due to the measurement errors, reliability coefficients are used to calculate the upper and lower limits of pickup currents. For example, the lower limit of a relay can be calculated as $K.I_n$; where K is the reliability coefficient that is set to 1.1...1.2 and I_n is the nominal current of the line [32].

On the other hand, in active distribution networks, the magnitude/direction of the lines current would be changed based on the variations in the operational conditions of the network. Therefore, a centralized adapting unit (CAU) has been designed to re-calculate the relays pickup currents according to the network operational conditions. The CAU calculates the new pickup currents based on the power flow equations of the DC systems presented in [33]. In a multi-terminal DC network, the power flow from the DC buses to the DC grid is given by:

$$\mathbf{P} = \boldsymbol{U} \otimes (\boldsymbol{YU}) \tag{1}$$

where the vector $\boldsymbol{U}$ denotes the busses voltages, $\boldsymbol{Y}$ denotes the admittance matrix of the grid, and $\otimes$ is the Hadamard product operator. The vectors $\boldsymbol{P}$ and $\boldsymbol{U}$ are introduced in (2).

$$\boldsymbol{P} = \begin{bmatrix} \mathrm{P}_1 \\ . \\ . \\ . \\ \mathrm{P}_n \end{bmatrix}, \qquad \boldsymbol{U} = \begin{bmatrix} \mathrm{U}_1 \\ . \\ . \\ . \\ \mathrm{U}_n \end{bmatrix} \tag{2}$$

Consequent to the change in the injected power to the DC busses, the DC voltage variation of the network can be obtained by:

$$\Delta\mathbf{U} = \mathbf{J}_{\mathrm{DC}}^{-1}\ \Delta\boldsymbol{P} \tag{3}$$

where $\Delta\boldsymbol{P}$ denotes the nodal power variation and $\mathbf{J}_{\mathrm{DC}}$ is the Jacobian matrix of the DC grid that is given by:

$$\mathbf{J}_{\mathrm{DC}} = \mathrm{diag}(\mathbf{U}) \cdot \mathbf{Y} + \mathrm{diag}(\mathbf{YU}) \tag{4}$$

substituting (4) into (3), the voltage of the DC busses after the change in nodal injected power are calculated by:

$$\mathbf{U}_2 = \mathbf{U}_1 + \mathbf{J}_{DC}^{-1}\ \Delta\mathbf{P} \qquad (5)$$

where, vectors $\boldsymbol{U}_1$ and $\boldsymbol{U}_2$ denote the voltages of DC busses before and after any event, respectively. Finally, the current of each DC feeder could be found by:

$$\mathbf{I} = \mathbf{Y} \cdot \mathbf{U}_2 = \mathbf{Y} \cdot (\mathbf{U}_1 + \mathbf{J}_{DC}^{-1}\ \Delta\mathbf{P}) \qquad (6)$$

The equation (6) illustrates that the connection/disconnection of DGs or change in their generated power, reflected in $\Delta\boldsymbol{P}$, may also result in significant changes in feeders currents. Thus, in order to calculate the new pickup currents, the CAU monitors: 1) the status of the DCCBs and isolators to estimate the network topology and to update the $\boldsymbol{Y}$ matrix; 2) the injected power by DGs; and 3) the voltage of the DC busses. Then, the CAU calculates the new pickup currents and communicates with CIRs and LPUs to apply new settings.

6. Real-Time Verification

In order to evaluate the effectiveness of the proposed protection strategy, considering the communication delay, the HIL approach has been used. Fig. 5 presents the HIL test-bed setup which was developed using the following devices: 1) a real-time digital simulator (OPAL-RT) that simulates the study network; 2) a PC as the command station (programming host) that develops the Matlab/Simulink models that will be executed on the simulator; 3) a development board (DK60 Beck Co.) which has been used to implement the proposed protection algorithms for CIRs and LPUs, and 4) a router that is used to connect all the setup devices in the same sub-network. More details about the HIL test-bed setup can be found in the previous work of the authors presented in [34].

In this setup, the DK60 board operates as a protection relay and communicates through the Ethernet ports with the other protection elements which have been simulated on the simulator. The protection signals are exchanged between the board and the simulator by use of the standard messages. In the following test cases, the exchanged signals are received at the destinations after a time delay which is associated to different delay sources like: *i*) data preparing (packaging) in the sending node; *ii*) opening data package in the destination node.

7. Case Studies

The performance of the proposed strategy is studied here in the context of three following cases. In all these cases it is assumed that a fault is triggered at $t = 1s$.

7.1. Case Study 1: Occurrence of a pole to pole (PP) fault at F1

To evaluate the performance of the proposed strategy, it is assumed that a low-impedance fault (R_F =1Ω) strikes the study system when the communication system is active. Assuming that all the DGs are connected and generate their nominal power, the threshold of LPU1, LPU2, LPU4, LPU5 and LPU6 are set on 480A, 60A, 90A, 60A and 180A, respectively.

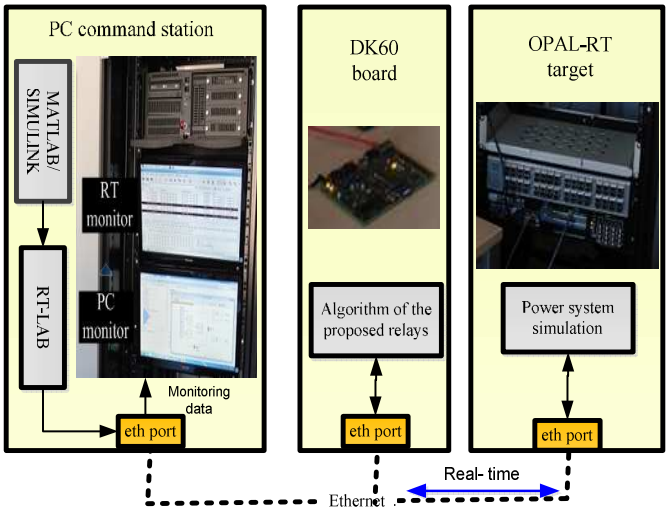

Fig. 5. *The components of the HIL setup.*

When the fault current reaches the threshold of the LPUs, they send trip commands to the corresponding DCCBs. For example, Fig. 6.a illustrates that LPU1 detects the fault and sends the trip command to DCCB1 around 0.1ms after the fault occurrence. During the operation of the DCCBs, the CIRs at both sides of each DC line exchange their DET and DIR signals to detect the faulty line. As measured form our experiments, CIR23 locates the faults around 2.7ms after the fault occurrence, as it is shown in Fig. 6.a. This relay, however, sends the open command to DIS23 when the current of this isolator decays to zero. Indeed, this test demonstrates that the time delay in fault location is around 2.7ms; hereafter, this time delay is referred to as T_D. Moreover, Fig. 6.b shows the fault current of VSC1 with and without external protection. This figure demonstrates that DCCB1 succeed to break the fault current before the critical time of VSC1. On other words, the external protection is fast enough to protect VSC1 and breaks the fault during the capacitor discharge period. Fig. 6.c shows the operational status of DCCB1 and DCCB6. The figure illustrates that although DCCB6 is located further away from the fault point, it works almost simultaneously with DCCB1.

The statuses of the other DCCBs (i.e., DCCB2, DCCB4 and DCCB5) are similar to those of the above mentioned DCCBs; hence, they were not displayed in this figure. Fig. 6.c also illustrates that 10ms after the fault clearance, DIS23 and DIS32 receive the open command form their CIRs. These two switches isolate the fault after 55-60ms, considering the use of conventional ACCBs as DC isolators. Once DIS23 and DIS32 are opened, CIR23 and CIR32 send the ISO signal to all the LPUs. Finally, the DCCBs are re-closed, when the LPUs received the ISO signals from CIR23 and CIR32. Fig. 6.c demonstrates that the rest of the study network is restored 85ms after the fault occurrence. The AC-side voltage of VSC1 during the fault isolation process is shown in Fig. 6.d. This figure demonstrates that the voltage of the AC network reaches to stability 2-3 cycles after the fault clearance.

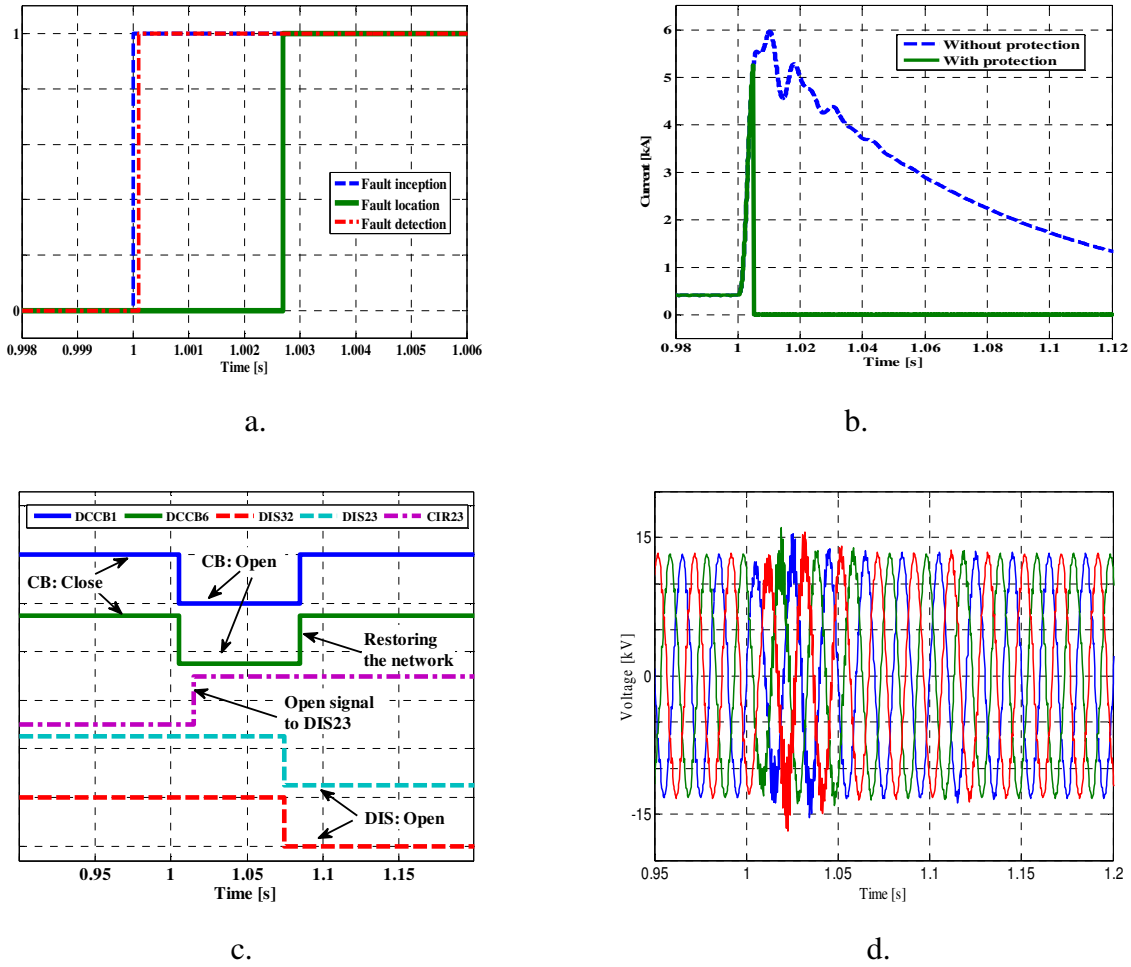

Fig. 6. *Results of Case Study1 (for a low-impedance fault).*

a. Fault detection time of LPU1 and fault location time of CIR23 (when R_F=1Ω).
b. Fault current of VSC1, with and without external protection.
c. Status of DCCB1, DCCB6, DIS23, DIS32, and CIR23's signal.
d. Voltage of the AC network (AC-side of VSC1).

Moreover, to consider the effect of the fault resistance on the performance of the proposed protection method, we assume that a high-impedance fault (R_F =100Ω) occurs at point F1. Fig. 7 shows that in this case, the fault is detected and located by CIR23 around 4.2ms after the fault occurrence; however, LPU1 cannot detect the fault during this time-interval. Indeed, in this case, the CIRs located at the both sides of the faulty line can detect the fault faster than the LPUs. Therefore, CIR23 sends a notification signal to the LPUs and then the LPUs send the trip commands to the corresponding DCCBs. Fig. 7 also illustrates that the rest of the protection steps are similar to the low-impedance fault cases.

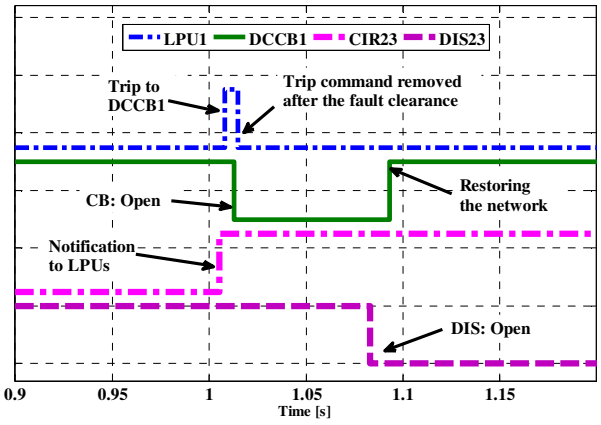

Fig. 7. *Status of LPU1, DCCB1, CIR23 and DIS23 for a high-impedance fault.*

7.2. Case Study 2: Occurrence of a PP fault at F1, when communication is interrupted.

In order to evaluate the backup protection, we assume that a PP fault impacts the network when the communication system is interrupted. In this case, the operation of the CIRs has been blocked and the algorithm for LPU2 has been implemented on the board. Similar to the first case study, at the first steps, the fault is detected by LPUs and the fault current is interrupted by the operation of the DCCBs. Moreover, the LPUs select the candidate isolators that should be opened. Since Bus3 was not equipped with LPU, the isolators connected to this bus remain closed. Furthermore, only one isolator has been connected to Bus5; thus, this isolator (DIS54) is the selected isolator for this bus. For the other busses, the isolator which carries the maximum positive current is selected. Fig. 8 shows the fault current of the isolators which are connected to each bus regardless of the operation of the protection devices. This figure demonstrates that according to the fault current flowing through the isolators, DIS12, DIS23, DIS43, and DIS64 are the selected isolators in Bus1, Bus2, Bus4, and Bus6, respectively. The selected isolators are opened after the fault current interruption. Fig. 9.a shows that DIS23 and DIS64 are completely opened almost 75ms after the fault occurrence; whereas, the status of DIS32 is not changed. To determine which isolators can be reclosed, the DCCBs are reclosed again and remain close for 100ms. During this time interval, DIS12 and DIS64 are selected as the isolators which can be closed.

The DCCBs are opened again 185ms after the fault occurrence, however the selected isolator, must be re-closed after the rated reclosing time (RRT). The RRT is related to the operational limitation of the conventional AC CBs and is 300ms for the fast-reclosing devices [35]. Therefore, the re-close command is applied to the selected isolators at $t = 1.375s$. Fig. 9.a shows that the study network is restored 470ms after the fault occurrence.

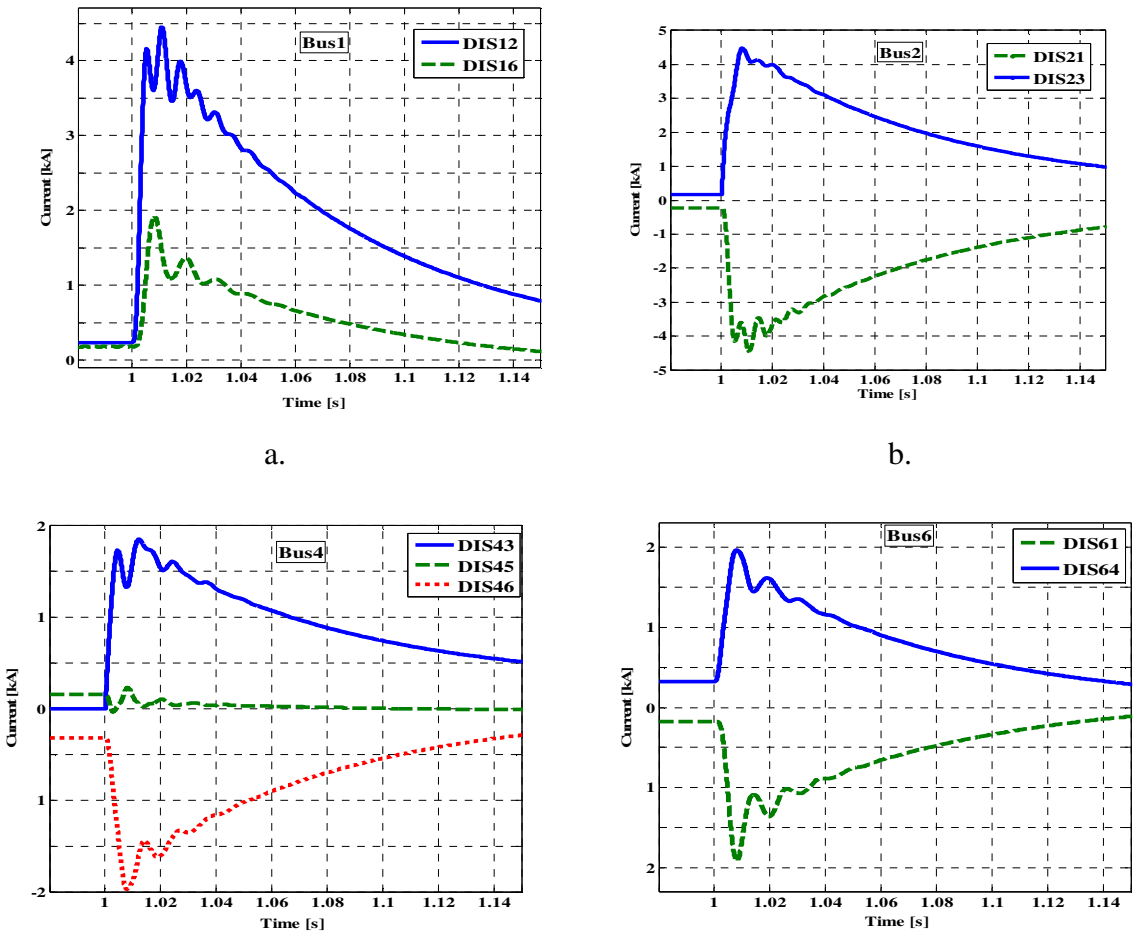

Fig. 8. *Fault currents flowing through isolators of different buses.*

a. Bus1. Maximum positive current flows from DIS12.
b. Bus2. Maximum positive current flows from DIS23.
c. Bus4. Maximum positive current flows from DIS43.
d. Bus6. Maximum positive current flows from DIS64.

7.3. Case Study 3: occurrence of a PP fault at F1, when a DC isolator fails to operate

To study the performance of the isolator-failure backup protection, this case study assumed that after the fault occurrence in Line23 and operation of the DCCBs, DIS23 fails to open. In this case, once CIR23, which is implemented on the board, detects that DIS23 cannot isolate the fault, sends the open command to DIS12 through CIR12. Moreover CIR23 sends a message to LPU2 to block the re-closing operation of DCCB2. Fig. 9.b shows that the backup signals are sent 70ms after the fault location (10ms more than the nominal operational time of the isolators). Moreover, Fig. 9.b shows the status of DCCB1, DCCB2, and DIS21, which determines that the study network is restored after 160ms.

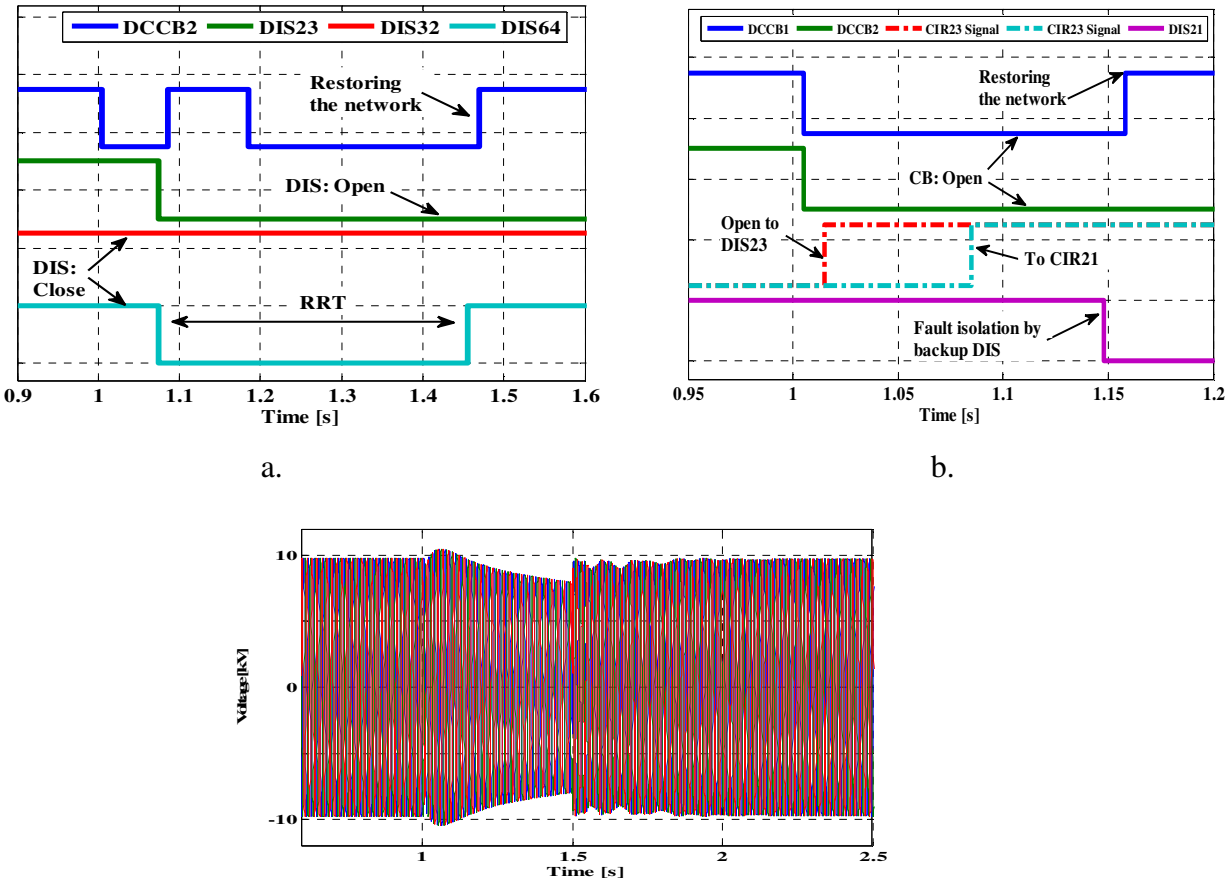

Fig. 9. *The DCCBs status for Case Studr2 and Case Study 3 and voltage of Microgrid1.*
a. The status of DCCB2, DIS23, DIS32, and DIS64 for Case Study 2.
b. The status of DCCB1, DCCB2, DIS21 and the signals of CIR23 to DIS23 and CIR21 for Case Study3.
c. Three phase voltage of the Microgrid-1's PCC.

8. Discussion

This section investigates the effects of the isolation process and the network restoration on the connected loads. The main protection method restores the network in less than 100ms; while the required time for the backup scheme is less than 500ms. These time delays are in the range of the momentary interruptions in AC distribution systems which happen due to the operation of auto-reclosers, sectionalizers and automatic network restoration process [36, 37]. Therefore, in the worst cases, the proposed method restores the network after a time delay which is in the range of the time delay of the existing system-restoration methods of AC distribution system. It is worth noting that, the power quality of DC distribution systems can be improved by replacing some of the isolators with DCCBs. For example, let's assume that in the network of Fig. 3, DIS12 and DIS43 have replaced with DCCBs. In this case, after the fault occurrence at point F1, it is not necessary to open all the DCCBs. Hence, only the loads and microgrids that are connected to Bus2 and Bus3 sense the momentary interruption. This change, can enhance the power quality; however, increase the costs of the protection system.

Furthermore, one of the most important applications introduced for the MVDC networks is connecting AC microgrids [22]. Loads inside the microgrids can be supported by DGs during the fault isolation. Therefore, these loads only face with a short-time voltage reduction (voltage sag). According to the ITIC curve and IEEE Std 1564-2014 [38] the voltage reduction limited to 70% of the nominal voltage does not cause any interruption even for the sensitive loads, if the voltage restores in less than 500ms. Simulation results show that, for the worst cases (i.e., when communication fails), this goal can be achieved for the microgrids of the study system when the generated power of DGs inside a microgrid at least reach to 50% of the connected load's power. For example, Fig. 9c shows the voltage of the main AC-bus of Microgrid-1 when DGs inside this microgrid generate 2.5 MW and all the loads were connected. This figure illustrates that the RMS value of the voltage drops to 70% of its nominal value. This voltage, however, returns to its nominal value after the network restoration. Therefore according to the ITIC curve presented in the IEEE Std 1564-2014, the sensitive loads do not perceive any momentary interruption.

9. Conclusions

This paper proposes an adaptive-communication-assisted protection strategy for MVDC networks. The fault clearance and isolation are achieved by the coordinated operation of DCCBs and isolator switches. The method is fast enough to interrupt the fault before damage to the VSC stations and adversely effects on the AC network. The HIL simulation results show that the main protection strategy works properly and restores the network in less than 85ms. This time is less than the typical network restoration time in AC distribution systems by use of CBs, auto-reclosers and sectionalizers. The paper also presents a fast, selective and reliable fault location method which is able to detect the faulty line without using complex calculations. Moreover, the intermittent nature of DGs and change in the network topology do not cause any protection blinding or mal-operation.

10. Appendix

Table 2. MVDC network parameters.

	DG's Power (MW)	**Load (MW)**
Bus2 (Microgrid1)	4	5
Bus3	-	3.5
Bus4	-	5
Microgrid2 (total)	5	3.5
Bus5	1	4
Bus6	3	-

Table 3. Network cable, equivalent π, model parameters.

DC line	Line12	Line23	Line30	Line34	Line40	Line45	Line46	Line16
R[Ω]	0.070	0.146	1.161	0.117	0.134	0.386	0.082	0.117
L[mH]	0.511	1.325	1.414	0.852	0.223	0.847	0.596	0.852
C[μF]	2.16	1.6	0.51	0.9	0.095	0.42	2.52	3.6

11. References

[1] Hajian, M., Jovcic, D., Bin, W.: "Evaluation of Semiconductor Based Methods for Fault Isolation on High Voltage DC Grids", *IEEE Trans. Smart Grid,* 2013, **4**, (2), pp. 1171-1179

[2] Fletcher, S.D.A., Norman, P.J., Galloway, S.J., *et al.*: "Optimizing the Roles of Unit and Non-unit Protection Methods Within DC Microgrids", *IEEE Trans. Smart Grid,* 2012, **3**, (4), pp. 2079-2087

[3] Monadi, M., Zamani, M.A., Candela, J.I., *et al.:* "Protection of AC and DC distribution systems Embedding distributed energy resources: A comparative review and analysis", *Renew. Sust. Energy Rev., 2015,* **51**, pp. 1578-1593

[4] Mohanty, R., Mukha Balaji, U.S., Pradhan, A.: "An Accurate Non-iterative Fault Location Technique for Low Voltage DC Microgrid", *IEEE Trans. Power Del.,* 2016*,* **31** , (2), pp. 475-481

[5] De Kerf, K., Srivastava, K., Reza, M., *et al.:* "Wavelet-based protection strategy for DC faults in multi-terminal VSC HVDC systems," *IET Gen. Trans. Dist.,2011,* **5**, (4), pp. 496-503

[6] Cairoli, P., Kondratiev, I., Dougal, R.A.: "Coordinated control of the bus tie switches and power supply converters for fault protection in dc microgrids", *IEEE Trans. Power Electron.,2013,* **28**, (4), pp. 2037-2047

[7] Jovcic, D., Taherbaneh, M., Taisne, J.P., *et al.:* "Topology assessment for 3 + 3 terminal offshore DC grid considering DC fault management", *IET Gen. Trans. Dist, 2015,* **9**, (3), pp. 221-230

[8] Tang, L., Ooi, B.T.: "Locating and isolating DC faults in multi-terminal DC systems", *IEEE Trans. Power Del.,2007,* **22**, (3), pp. 1877-1884

[9] Yang, J., Fletcher, J.E., O'Reilly, J.: "Short-circuit and ground fault analyses and location in VSC-based DC network cables," *IEEE Trans. Ind. Electron.,2012 ,* **59**, (10), pp. 3827-3837

[10] Park, J.D., Candelaria, J., Ma, L.Y., *et al.*: "DC Ring-Bus Microgrid Fault Protection and Identification of Fault Location", *IEEE Trans. Power Del.,2013,* **28**, (4), pp. 2574-2584

[11] Leterme, W., Beerten, J., Van Hertem D.: "Non-unit protection of HVDC grids with inductive dc cable termination," *IEEE Trans. Power Del.,*2016, **31**, (2)*,* pp. 820-828

[12] Salomonsson, D., Soder, L., Sannino, A.: "Protection of low-voltage DC microgrids," *IEEE Trans. Power Del.,2009,* **24**, (3), pp. 1045-1053

[13] Baran, M. E., Mahajan, N.R.: "Overcurrent protection on voltage-source-converter-based multiterminal DC distribution systems", *IEEE Trans. Power Del.,* 2007, **22,** (1), pp. 406-412

[14] Farhadi, M., Mohammed, O.A.: "Event-Based Protection Scheme for a Multiterminal Hybrid DC Power System," *IEEE Trans. Smart Grid,* 2015, **6**, (4), pp. 1658-1669

[15] Christopher, E., Sumner, M., Thomas, D.W.P., *et al.*: "Fault Location in a Zonal DC Marine Power System Using Active Impedance Estimation", *IEEE Trans. Ind. App.,* 2013, **49**, (2), pp. 860-865

[16] Chanda, N.K., Fu, Y.: "ANN-based fault classification and location in MVDC shipboard power systems," Proc. *North American Power Symposium, 2011*, pp. 1-7.

[17] Li, W.L., Monti, A., Ponci, F.: "Fault Detection and Classification in Medium Voltage DC Shipboard Power Systems With Wavelets and Artificial Neural Networks", *IEEE Trans. Instru. Measur., 2014,* **63**, (11), pp. 2651-2665

[18] Jingzhou, C., Minyuan, G., Lv, T., *et al.*: "Paralleled multi-terminal DC transmission line fault locating method based on travelling wave", *IET Gen. Trans. Dist,2014,* **8**, (12), pp. 2092-2101

[19] Azizi, S., Afsharnia, S., Sanaye-Pasand, M.:"Fault location on multi-terminal DC systems using synchronized current measurements", *Inter. Jour. Elec. Power Energy Syst., 2014,* **63**, pp. 779-786

[20] Fletcher, S.D.A., Norman, P.J., Fong, K., *et al.*: "High-Speed Differential Protection for Smart DC Distribution Systems", *IEEE Trans. Smart Grid, 2014,* 5, (5), pp. 2610-2617

[21] Abu-Elanien, A.E.B., Elserougi, A.A., Abdel-Khalik, A.S., *et al.*: "A differential protection technique for multi-terminal HVDC", *Elec. Power Syst. Res., 2016,* **130**, pp. 78-88

[22] Majumder, R.:"Aggregation of microgrids with DC system," *Elec. Power Syst. Res.,* 2014,**108**, pp. 134-143

[23] Justo, J.J., Mwasilu, F., Lee, J., *et al.*: "AC-microgrids versus DC-microgrids with distributed energy resources: A review", R*enew. Sust. Energy Rev.,* 2013, **24**, pp. 387-405

[24] Larruskain, D.M., Zamora, I., Abarrategui, O., *et al.*: "Conversion of AC distribution lines into DC lines to upgrade transmission capacity", *Elec. Power Sys. Res., 2011,* **81**, pp. 1341-1348

[25] Larruskain, D.M., Zamora, I., Abarrategui, O., et al.: "VSC-HVDC configurations for converting AC distribution lines into DC lines", *Inter. Jour. Elec. Power Energy Syst.,2014,* **54**, pp. 589-597
[26] Baran, M.E., Mahajan, N.R.: "DC distribution for industrial systems: opportunities and challenges"*, IEEE Trans. Ind. App., 2003,* **39**, (6), pp. 1596-1601
[27] Franck, C.M.:"HVDC Circuit Breakers: A Review Identifying Future Research Needs," *IEEE Trans. Power Del.,2011,* **26,** (2), pp. 998-1007
[28] Sneath, J., Rajapakse, A.D.: "Fault Detection and Interruption in an Earthed HVDC Grid using ROCOV and Hybrid DC Breakers", *IEEE Trans. Power Del.,2014,* ***29***, pp. 1-8
[29] Callavik, A.B.M., Häfner, J., Jacobson. B.: "The Hybrid HVDC Breaker: An innovation breakthrough enabling reliable HVDC grids" [Online].
[30] Hassanpoor, A., Hafner, J., Jacobson, B.: "Technical Assessment of Load Commutation Switch in Hybrid HVDC Breaker", *IEEE Trans. Power Electron.,2015,* **30**, (10), pp. 5393-5400
[31] "Gas insulated MV circuit-breakers," in *Medium voltage products*, ABB, Ed., ed: www.abb.com, 2013.
[32] Anderson, P.M.:"*Power system protection",* McGraw-Hill New York, 1999.
[33] Haileselassie, T.M., Uhlen, K.: "Impact of DC Line Voltage Drops on Power Flow of MTDC Using Droop Control", *IEEE Trans. Power Syst., 2012,* **27**, (3), pp. 1441-1449
[34] Monadi, M., Koch-Ciobotaru, C., Luna, A., *et al.*: "A protection strategy for fault detection and location for multi-terminal MVDC distribution systems with renewable energy systems", *Proc. Int.* Conf. *Renew. Energy Res. App,* 2014, pp. 496-501.
[35] *ANSI C37.06-2000:* "American National Standard for AC High-Voltage Circuit Breakers - Rated on a Symmetrical Current Basis - Preferred Ratings and Related Required Capabilities"*,* 2003
[36] Anwar, A., Yucheng, Z., Brice, C.W., *et al.*: "Soft Reclosing of an Industrial Power Network Using an Inverter-Controlled Energy-Storage System", *IEEE Trans. Power Del., 2014,* **29**, (3), pp. 1111-1119
[37] Eriksson, M., Armendariz, M., Vasilenko, O.O., *et al.*: "Multiagent-Based Distribution Automation Solution for Self-Healing Grids", *IEEE Trans. Ind. Electron., 2015,* **62**, (4), pp. 2620-2628
[38] *IEEE Std 1564-2014:* "IEEE Guide for Voltage Sag Indices"*,* 2014